Mechanisms of Locking of the El Niño and La Niña Mature Phases to Boreal Winter*

SOON-IL AN AND BIN WANG

International Pacific Research Center, School of Ocean and Earth Science and Technology, University of Hawaii at Manoa, Honolulu, Hawaii

(Manuscript received 19 April 2000, in final form 5 September 2000)

ABSTRACT

The peaks of El Niño in the Cane–Zebiak (CZ) model tend to appear most frequently around November when the ocean Rossby waves, which were amplified during the previous unstable season (February–May), turn back to the eastern Pacific and when the local instability in the eastern Pacific is very weak. The peaks of La Niña in the CZ model occur most frequently in boreal summer, in contrast to the observed counterpart that usually occurs in boreal winter. Sensitivity experiments indicate that the phase locking of the La Niña to boreal summer is primarily caused by seasonal variations of the tropical convergence zone, which regulate convective heating through atmospheric convergence feedback. The observed thermocline and the wind anomalies in the western Pacific exhibit considerable seasonal variations. These were missed in the original CZ model. In a modified CZ model that includes the seasonal variations of the western Pacific wind anomalies and the basic-state thermocline depth, the peaks of La Niña preferably occur in boreal winter, suggesting that the seasonal variation of the western Pacific surface wind anomalies and the mean thermocline depth are critical factors for the phase locking of the mature La Niña to boreal winter. The mechanisms by which these factors affect ENSO phase locking are also discussed.

1. Introduction

The interaction of El Niño–Southern Oscillation (ENSO) with the annual cycle has been recognized as the fundamental cause of deterministic chaos and frequency and phase locking to the annual cycle (Jin et al. 1994; Tziperman et al. 1994; Tziperman et al. 1995; Chang et al. 1994, 1995; Wang and Fang 1996; Jin 1996; Wang et al. 1999a). The observed ENSO index, the Niño-3 (5°S–5°N and 150°–90°W) SST anomaly obtained from Kaplan SST data (Kaplan et al. 1998), which covers the period from 1856 to 1992, shows that the peaks of both El Niño (warm event) and La Niña (cold event) tend to occur toward the end of a calendar year from November to January (Fig. 1c). The analyses of the Comprehensive Ocean–Atmosphere Data Set yield similar results (e.g., Chang et al. 1995). The phase locking of El Niño and La Niña peaks to boreal winter is one of the most robust features of ENSO cycles.

The Cane–Zebiak model (hereafter CZ; Cane and Zebiak 1985; Zebiak and Cane 1987), a pioneering intermediate class coupled model for simulation of ENSO, has been widely used for understanding of the basic mechanism and predictability of ENSO (e.g., Cane et al. 1986; Zebiak and Cane 1987; Goswami and Shukla 1993; Mantua and Battisti 1995; Tziperman et al. 1995, 1997; Chen et al. 1998; An and Wang 2000). The CZ model predicts anomalous quantities by prescribing basic states of the atmosphere and ocean including the surface winds (U, V) and divergence (DIV), ocean surface layer currents (u, v), and the upwelling (w) at the base of the surface layer, sea surface temperature (SST), vertical SST gradients at the bottom of the surface layer, and thermocline depth (H). Thus, the CZ model is convenient for studying impacts of the basic-state seasonal cycles on ENSO, although it neglects the feedback of ENSO to the mean state.

In the CZ model, the phase locking of El Niño to the annual cycle is due to seasonally varying basic states. As shown in Fig. 2c, when the annual cycles of the basic-state parameters (U, V, DIV, u, v, w, and SST) were included, the simulated El Niño tends to mature around November (in this experiment, we increased the coupling coefficient by 20% of the original value). However, when the annual mean basic states were specified, the peaks of El Niño and La Niña appeared randomly during the course of the calendar year (Fig. 2d). Al-

* School of Ocean and Earth Science and Technology Contribution Number 5334 and International Pacific Research Center Contribution Number IPRC-76.

Corresponding author address: Dr. Soon-Il An, International Pacific Research Center, SOEST, University of Hawaii at Manoa, Honolulu, HI 96822.
E-mail: sian@soest.hawaii.edu

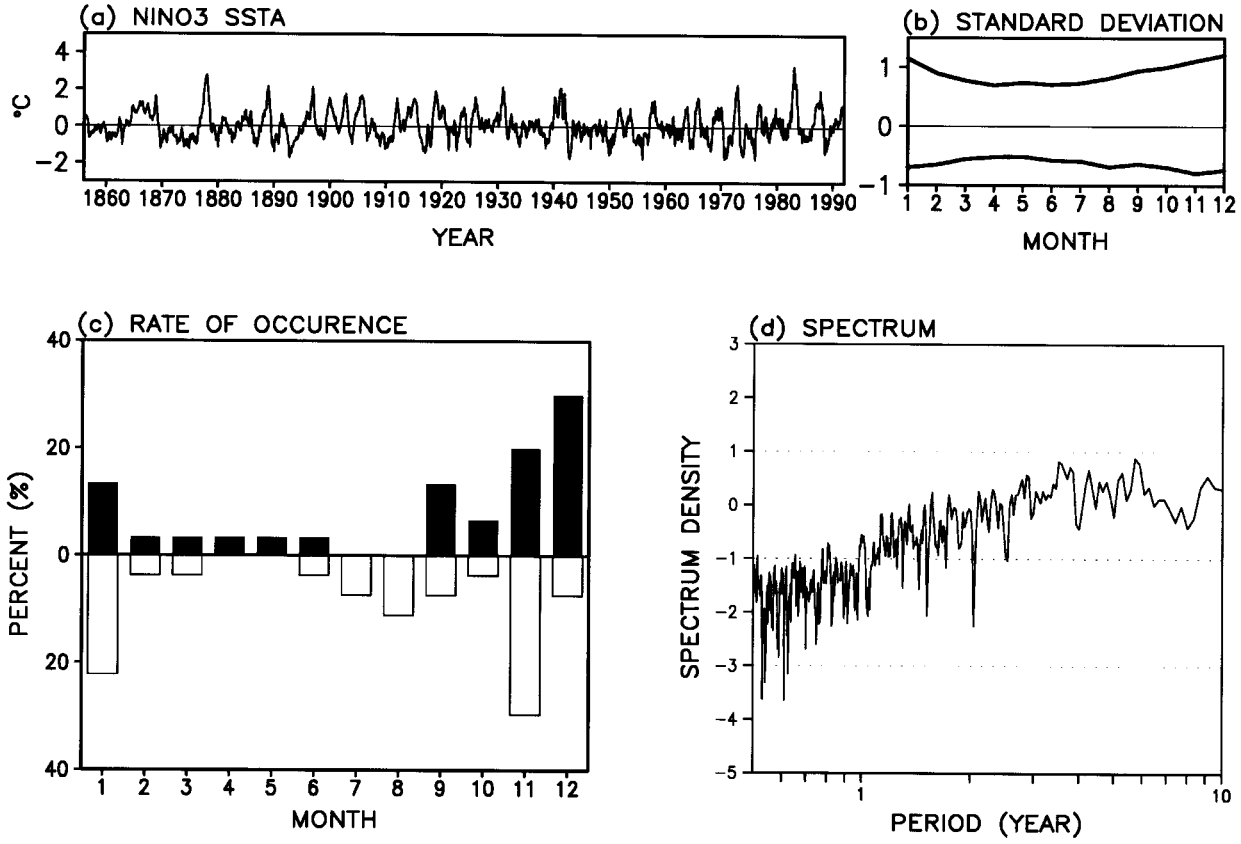

FIG. 1. (a) Time series of the observed SST anomaly over the Niño-3 region (5°S–5°N and 90°–150°W) obtained from Kaplan et al. (1998). (b) Standard deviation of Kaplan's Niño-3 SST anomaly for each calendar month. (c) Histograms of the rate of occurrence of El Niño (filled bar) and La Niña (blank bar) peaks for each calendar month. The percentage is calculated by the ratio of the numbers of El Niño (La Niña) peaks for each calendar month divided by the total numbers of El Niño (La Niña) peaks. (d) Spectral density distribution of Kaplan's Niño-3 SST anomaly.

though the CZ model simulates the occurrence of peak phases of El Niño reasonably well, the peaks of La Niña events occur most frequently in boreal summer, which is at odds with observation (from November to January). The cause has not been understood.

Tziperman et al. (1998) explained why the peaks of El Niño occur in boreal winter based on the delayed oscillator theory. They pointed out that seasonally varying amplification of Rossby and Kelvin waves due to coupled instability forces an event to mature when this amplification is at its minimum strength, at boreal winter. However, the phase-locking mechanism of La Niña has not been explained. Since the impacts of La Niña on the global climate tend to be opposite to and as prominent as those of El Niño (Ropelewski and Halpert 1987, 1989; Deser and Wallace 1990), study of the seasonal phase lock of La Niña is important and may further improve our understanding of the basic dynamics of the ENSO cycle.

In addition to the mechanisms existing in the CZ model, other processes might also be important. For instance, anomalous surface winds in the western North Pacific associated with ENSO have significant seasonality, which has been suggested as a factor in the ENSO phase transition (Harrison and Vecchi 1999; Wang et al. 1999b). However, as shown in Fig. 3, the atmospheric component of the CZ model is not able to reproduce the observed wind anomalies in the western North Pacific (Figs. 3a and 3b). Second, the equatorial thermocline depth is a critical parameter in the CZ model, because the mean thermocline depth influences the model results through change of subsurface temperature anomalies. The mean thermocline depth in the CZ model is prescribed as a function of longitude only and without seasonal variations. In reality, the meridional variation of the mean thermocline depth is prominent, and the amplitude of the seasonal displacement of the equatorial thermocline in the eastern and central Pacific exceeds 10 m (Fig. 4b). The possible impacts of the aforementioned factors need to be explored.

In this study, using the Cane–Zebiak model (CZ model) and a modified version, we examine mechanisms responsible for both the El Niño and La Niña phase locking with emphasis on the La Niña events. In section 2, we first reexplore the cause of the phase locking of ENSO in the CZ model, in particular, the seasonal effect

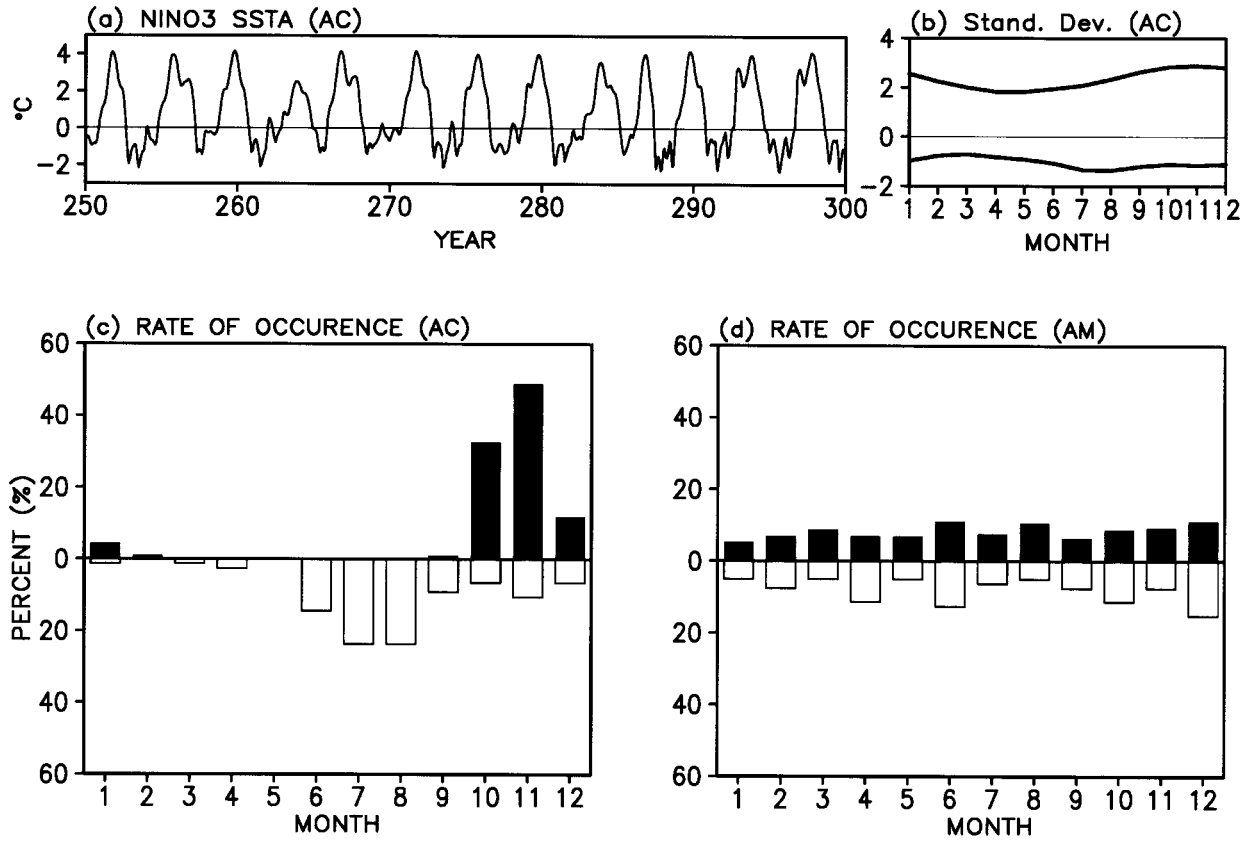

FIG. 2. (a)–(c) The same as in Figs. 1a–c except that the Niño-3 SST anomalies were derived from a 300-yr integration of the Cane–Zebiak model with the annual cycle basic states. For clarity, only the last 50 yr are shown in (a). (d) The same as in (c) except that in the Cane–Zebiak model the annual mean basic states were used.

of the wind divergence. In section 3, a modified CZ model (MOD-CZ model) is developed, in which the seasonal effects of the surface winds in the western North Pacific and the thermocline displacement are included. Using the MOD-CZ model, we assess the impacts of the seasonal effects of the prescribed oceanic and atmospheric basic states on the ENSO phase locking. The concluding remarks are given in section 4.

2. The ENSO phase locking in the Cane–Zebiak model

Tziperman et al. (1998) argued that one of the reasons for the locking of El Niño peak to boreal winter is that the seasonally varying amplification of the Rossby and Kelvin waves by coupled instability forces the El Niño to mature at the time when the amplification reaches minimum strength, at the end of the calendar year. In boreal winter, owing to weak coupled instability the effect of Kelvin waves balances that of the reflected Rossby waves that were generated from highly amplified Rossby waves during the previous summer.

Our experimental results support the above argument. To identify the impacts of the basic-state annual cycle in an individual month on ENSO cycles, we fixed basic states at annual mean values except for a particular month during which the annual departure of the basic states is added. As shown in Figs. 5b–e, El Niño reaches a peak in boreal winter when the annual departure was turned on during the period of February–May (defined as type 1). Based on the monthly instability index shown in Fig. 4 of Tziperman et al. (1998), it is suggested that the annual departure in February–May makes the basic state unstable. As mentioned in Tziperman et al. (1998), during a month in which the coupled instability of the basic state is strong, the timing of an El Niño peak may be determined by the timing of that month plus a lag of about 10 months. When the annual departure of the basic state is applied to the period from February to May, the peak season of El Niño changes from December to March (Figs. 5b–e). The timing of the annual departure of the basic state indeed leads the peak season of El Niño by about 10 months. It suggests that the boreal spring unstable basic states cause phase locking of El Niño through a remote reflection process, known as the delayed oscillator mechanism.

In this set of experiments, another type of El Niño phase lock (termed type 2) was also found, that is, the El Niño tends to mature in the same month when the

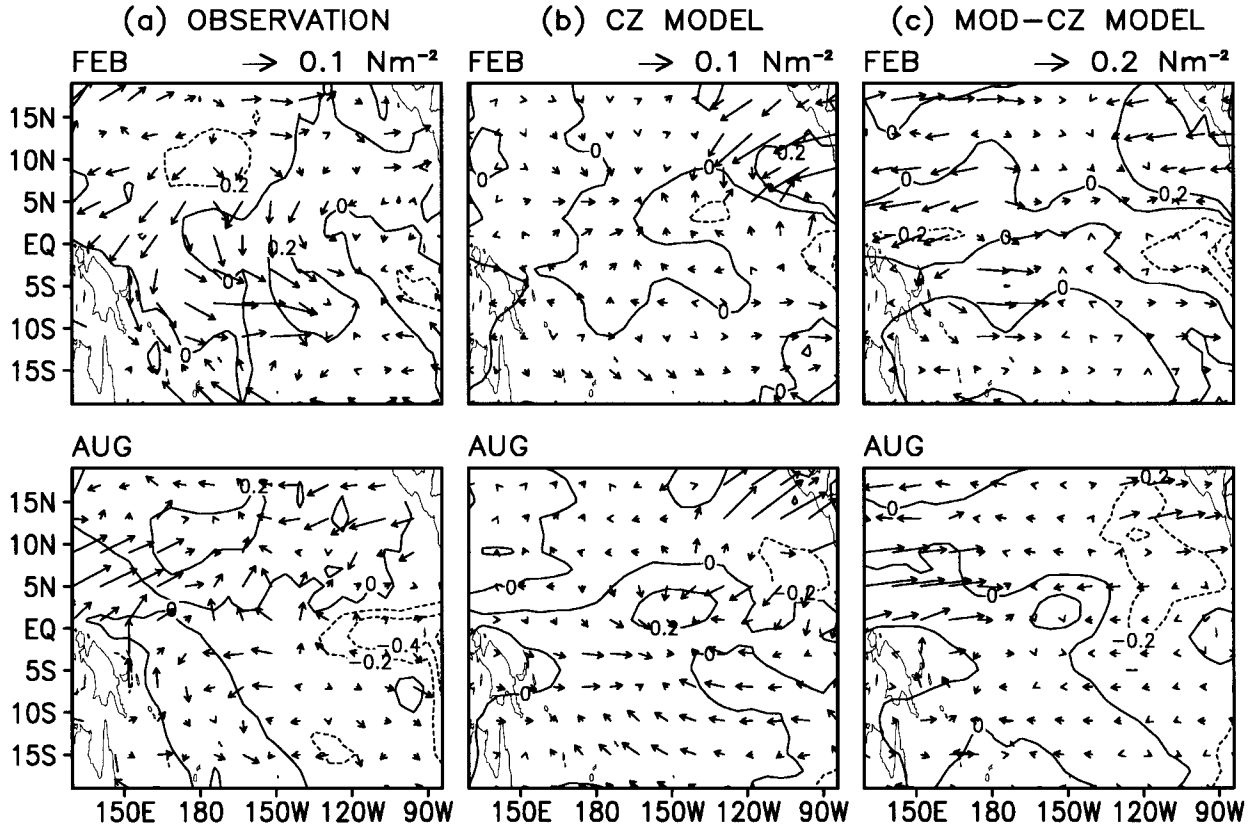

FIG. 3. The annual cycle component of the first SVD vectors of surface wind stress and SST anomalies derived from (a) observations, (b) the CZ model control run, and (c) the modified CZ model control run. To save space, the results are shown only for (top) Feb and (bottom) Aug. The SVD analyses were performed for each calendar month. The vector scale is displayed at the top right corner of each figure.

annual departure of the basic state is included. This type of phase locking happens when the annual departure is added from August to November (Figs. 5h–k). Note that, contrary to the unstable condition during February–May, the seasonal departure in August–November makes the basic state more stable than the annual mean (AM) basic state. This suggests that the type 2 phase locking of El Niño may be attributed to immediate depression of the growth of El Niño arising from reduction of a local air–sea coupled instability. It appears that a combination of the remote (type 1) and local (type 2) processes determines the phase locking of El Niño to boreal winter.

In the CZ model, there is a tendency for La Niña peak to occur in boreal summer from May to August irrespective of the seasonal dependence of the coupled instability (see Fig. 5). The La Niña shows a different behavior from the El Niño in terms of phase locking. It suggests that the cause of La Niña phase locking may differ from that of the El Niño. Such a difference might be due to the fact that nonlinear evolution of a warm perturbation differs from that of a cold one. In the CZ model, the major sources that could possibly cause different characteristics between an El Niño and a La Niña include, but are not limited to, the asymmetric parameterization of subsurface temperature with respect to warm and cold departure and the nonlinear atmosphere heating due to the convergence feedback acting as a switch on–off function [see the appendix of Zebiak and Cane (1987)]. The asymmetric parameterization of subsurface temperature is not directly related to the seasonal effect, because the mean thermocline depth in the CZ model does not have the seasonal variation. On the other hand, the nonlinearity in the heating parameterization is directly linked to the seasonal cycle of the surface wind convergence. Thus, it is expected that the seasonal variation of the convergence feedback might be correlated to the phase lock behavior of La Niña.

Tziperman et al. (1997) found that the seasonal phase locking of El Niño is dominated by the basic-state wind divergence associated with the seasonal march of the intertropical convergence zone (ITCZ), which regulates atmospheric heating. Additionally, the annual cycles of the background SST and ocean upwelling velocity were suggested as of second-order importance. To identify which mean states are most responsible for the phase locking, Tziperman et al. (1997) performed sensitivity tests, in which all basic states are fixed at the AM value

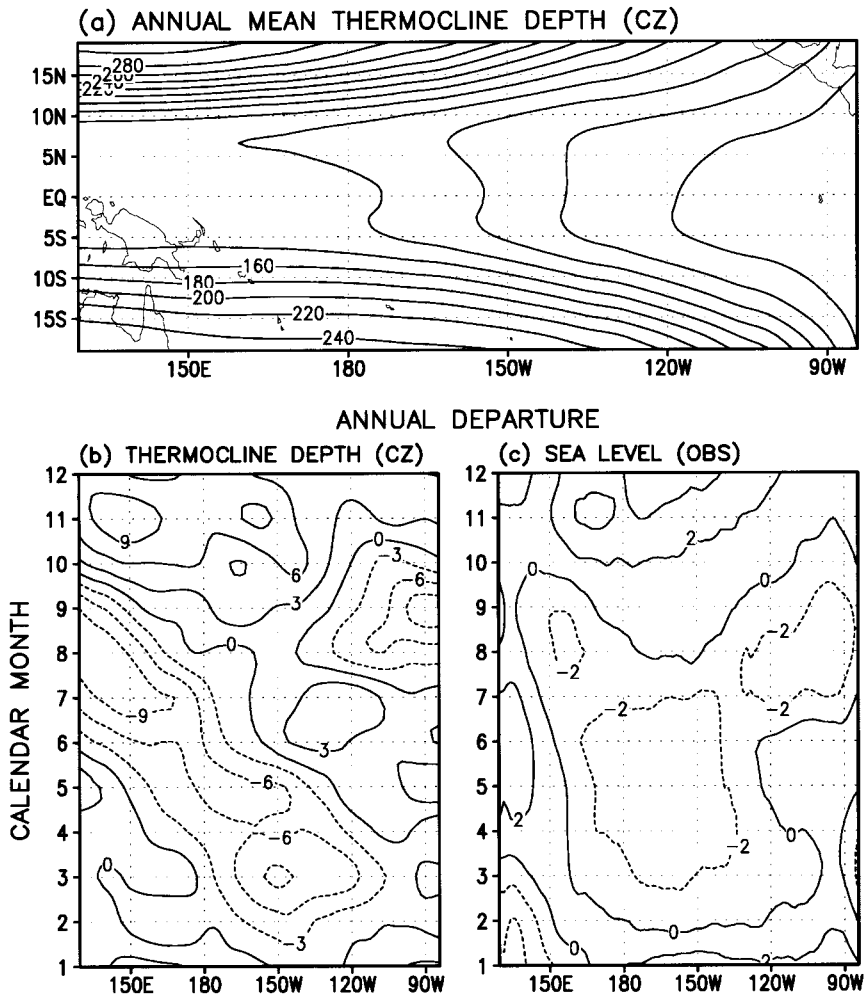

FIG. 4. (a) Annual mean thermocline depth obtained from the CZ ocean model forced by the basic-state wind stress used in the original CZ model. (b) Time–latitude cross section of the seasonal departure of the thermocline depth from its annual mean in the CZ model averaged over 1°S–1°N. (c) As in (b) except for the sea level height obtained from NCEP ocean assimilation data (Ji et al. 1995). Contour intervals are 20 m in (a), 3 m in (b), and 2 cm in (c).

except for one variable that retains annual cycle (AC). We have repeated the experiments in a way similar to those of Tziperman et al. (1997) except that the coupling coefficient, μ, increases from 1.0 to 1.2, where the coupling coefficient indicates the multiple factor for the drag coefficient. When the basic-state atmospheric divergence is specified as AC and all others as AM (Fig. 6a), both the El Niño and La Niña show a weak tendency of preferred occurrences from May to November, suggesting that the wind divergence may not be critical to the phase locking of ENSO cycle to the annual cycle. To further check the robustness of this result from a different perspective, we performed a complementary experiment in which the mean atmospheric divergence is specified as AM and all others as AC (Fig. 6b). If the wind divergence plays an important role, the phase locking is expected to weaken or change. Different from this expectation, the phase locking in this experiment is similar to that in the control experiment shown in Fig. 2c. Besides, the La Niña shows a more realistic phase locking to AC compared with the control experiment, because the largest frequency of occurrence appears in December, in a better agreement with the observation. The results suggest that the seasonal variation of the basic-state wind divergence does not affect the phase locking of El Niño significantly, while it plays a destructive role in the phase locking of La Niña in the CZ model.

Note that we used a larger coupling coefficient than that used in the standard CZ model, which we think is responsible for the difference between our results and Tziperman et al.'s (1997), because the models and numerical experimental design are basically the same. This suggests that effects of the seasonal variation of the basic-state atmospheric divergence may be sensitive to the coupling coefficient.

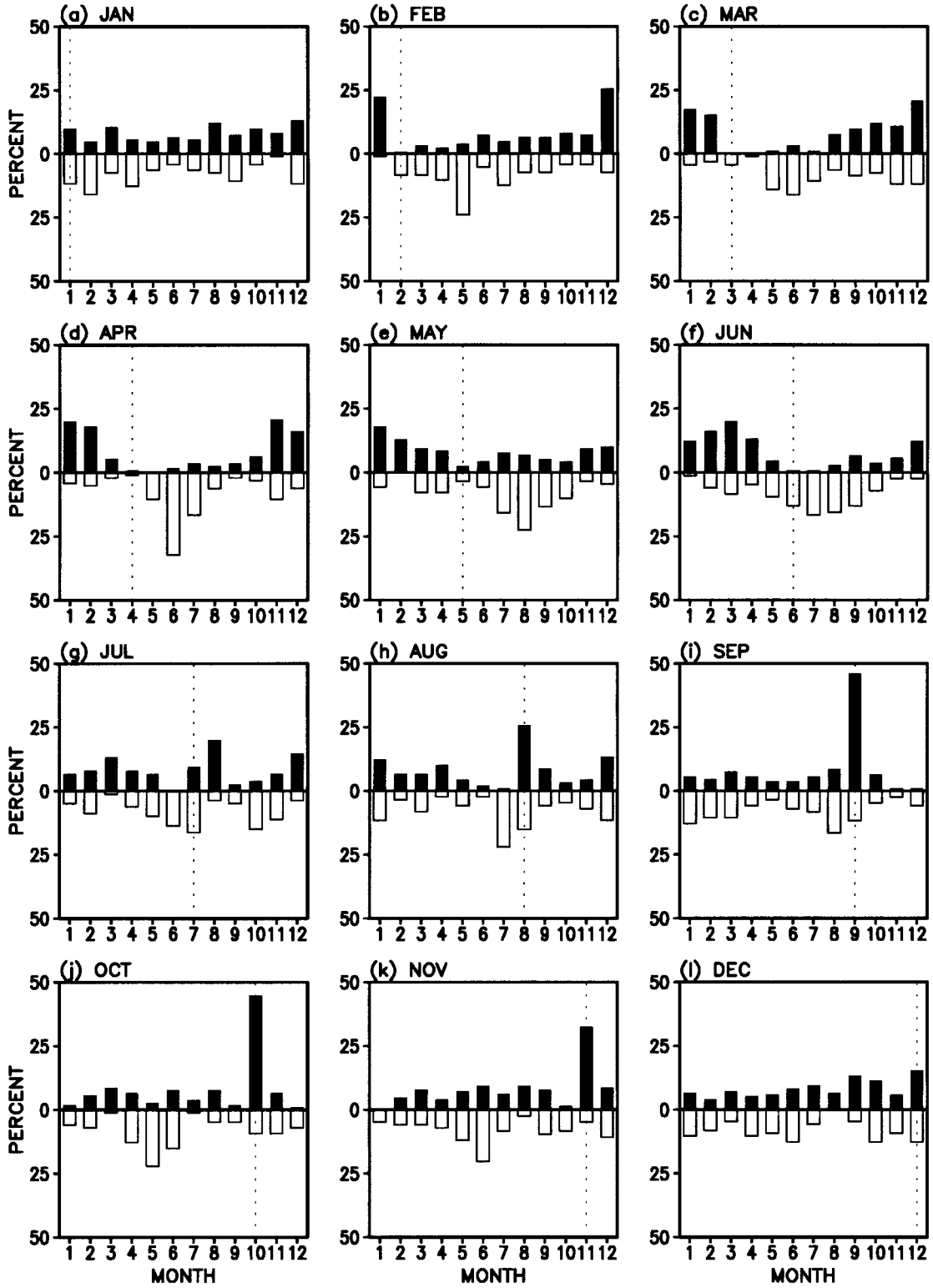

FIG. 5. Histograms showing the rate of occurrence of El Niño (filled bar) and La Niña (blank bar) peaks in the standard CZ model (coupling coefficient $\mu = 1.0$) with the basic states being fixed at annual mean values for all calendar months except that for the calendar month indicated at the upper-right corner of each panel the basic states have an annual departure.

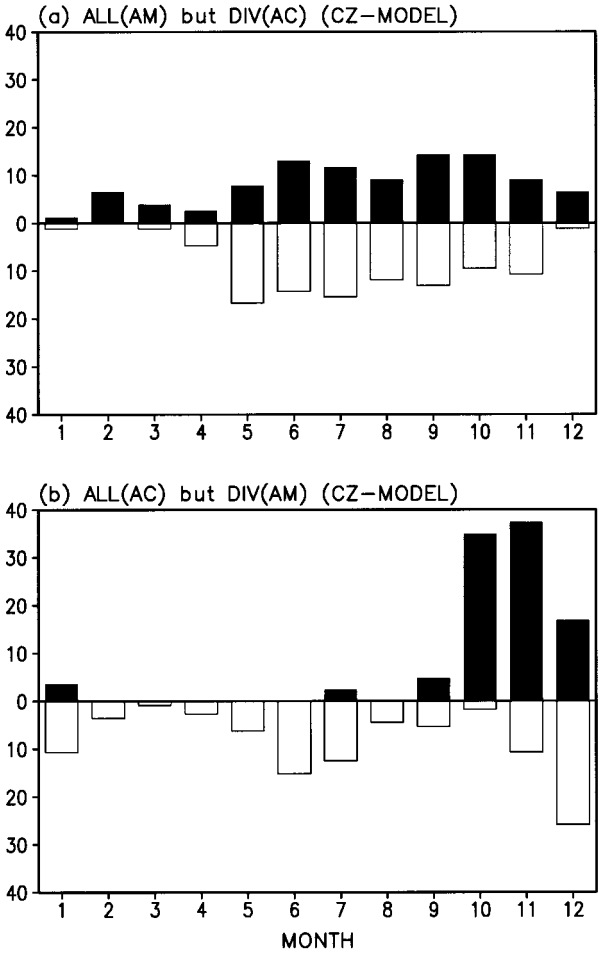

FIG. 6. Histograms showing the rate of occurrence of El Niño (filled bar) and La Niña (blank bar) peaks in the standard Cane–Zebiak model (coupling coefficient $\mu = 1.2$) for each calendar month. (a) All basic-state parameters have AC except the surface wind divergence. (b) All basic-state parameters are fixed at their AM values except that the surface wind divergence has annual variations.

The atmospheric heating (Q_c) due to the convergence feedback in CZ model is given by

$$Q_c = L_c[M(C_m + C) - M(C_m)], \qquad (1)$$

here C is the convergence of the surface wind ($-\nabla \cdot \mathbf{V}$), and the subscript m indicates the basic state, L_c, is the latent heating parameter due to the moisture convergence, and $M(x)$ is x for $x > 0$, otherwise $M(x) = 0$. As indicated in Eq. (1), Q_c is a nonlinear function. Thus, it functions in a different way during an El Niño and a La Niña. This is because the anomalous surface wind convergence due to a warm SST anomaly during El Niño can provide an additional heating regardless of the basic-state surface wind divergence field, provided the anomalous convergence is larger than the basic-state divergence. On the other hand, an anomalous divergence due to a cold SST anomaly during La Niña can produce an additional cooling only in the region where the basic-state winds converge. Figures 7b and 7c show the evolution of the atmospheric heating due to convergence feedback (Q_c) during El Niño and La Niña, respectively. Results in Figs. 7b and 7c were the composite of 6 strong El Niño and La Niña events that appeared in the standard CZ model run, respectively. As shown in Fig. 7b, the positive Q_c for the El Niño composite tends to be confined in the near-equatorial region during boreal spring and summer when the mean divergence in the equatorial region is relatively weak, and then moves up to the off-equatorial region in the eastern North Pacific during November when the ITCZ locates furthest away from the equator. This results in the northward moving of Q_c, and the mean divergence is intensified resulting in the weakening of Q_c along the equator (Fig. 7a). On the other hand, the Q_c for the composite La Niña (Fig. 7c) shows a horseshoe shape. Its maximum appears during July and then moves to the west in August. Such a movement of the cooling center might be related to the evolution of the basic-state atmospheric divergence (Fig. 7a). Because, during that period, the equatorially symmetric mean convergence also moves westward from the eastern Pacific to the central–western Pacific. Note that this season-dependent movement of the anomalous surface wind divergence during the La Niña and associated resultant surface wind can also be responsible for westward propagation of the cold SST anomalies. Here, the cold SST anomalies are mainly due to the cold advection by westward currents generated by the wind stress change. This is a possible mechanism that differs from that arising from the surface layer feedback suggested by Jin and Neelin (1993).

In the La Niña case, the movement of atmospheric cooling due to the anomalous surface wind divergence during boreal summer may damp the cold perturbation. The reason follows. When the atmospheric cooling arrives at the western Pacific, two atmospheric cooling centers exist simultaneously: one is due to the surface wind divergence in the western Pacific and the other is due to the cold SST anomaly in the eastern Pacific. In the central Pacific, the westerly anomalies driven by the atmospheric cooling in the western Pacific and the easterly anomalies driven by that in the eastern Pacific cancel each other. As a result, the surface winds in the central Pacific are rapidly damped, resulting in a decay of the cold perturbation. This is why the peaks of La Niña frequently appear during boreal summer. On the other hand, during an El Niño, since the atmospheric heating due to convergence feedback provides an additional heating in the warming region, the warming would not decay during the boreal summer.

3. The ENSO phase locking in a modified Cane–Zebiak model

As mentioned in the introduction, the seasonality of the anomalous surface winds in the western North Pacific and the annual variation of the basic-state ther-

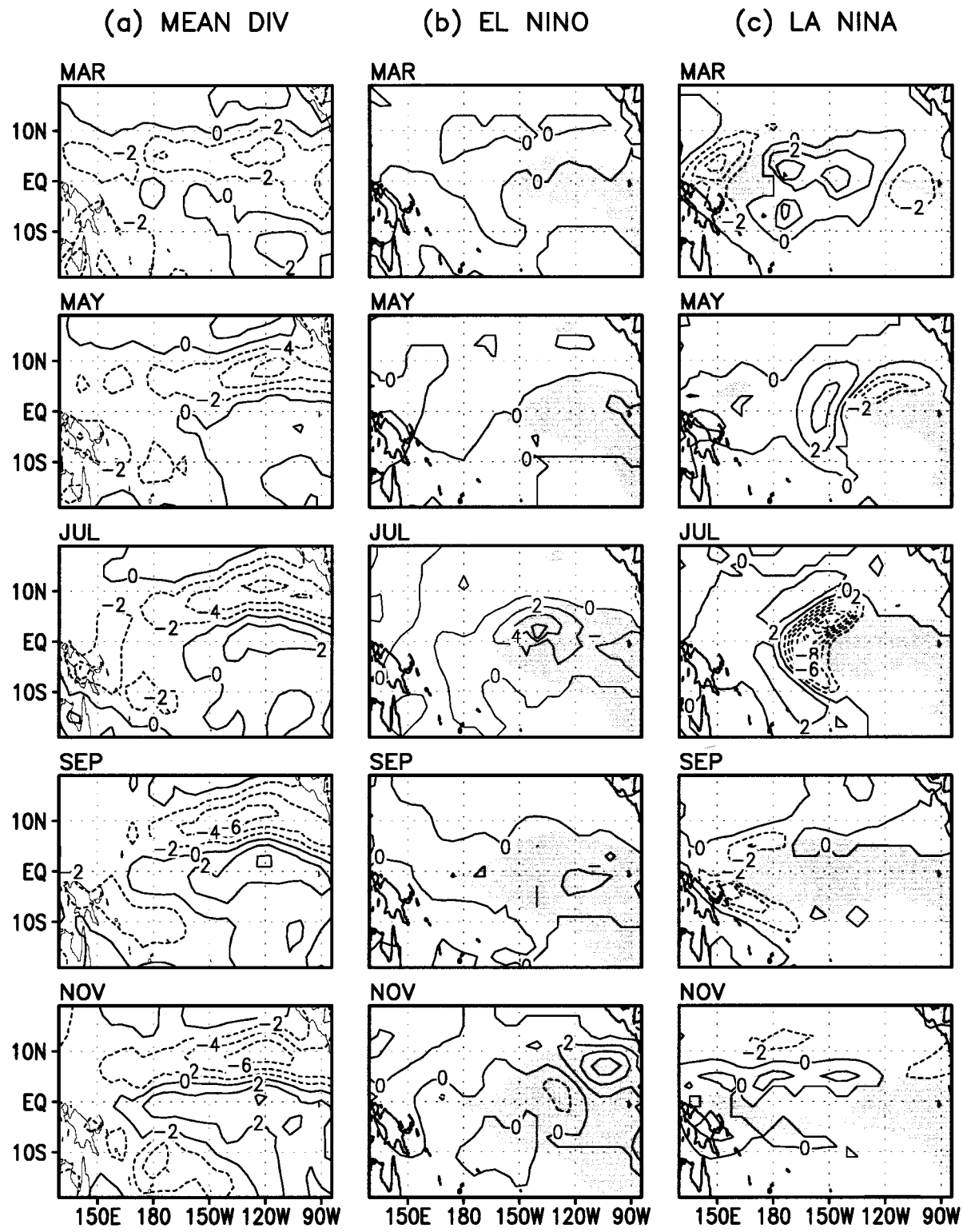

FIG. 7. (a) Basic-state atmospheric divergence used in the CZ model. (b) Anomalous atmospheric heating due to the convergence feedback during El Niño. (c) Same as in (b) except for La Niña. The shaded area in (b) and (c) indicates regions where SST anomalies are more than 1°C and less than −1°C, respectively. Units are 10^{-6} s^{-1} in (a), and 10^{-3} m^2 s^{-3} in (b) and (c). Each El Niño and La Niña evolution is derived from a composite of six prominent events appeared in the standard CZ model run. The time sequence is indicated in the upper-right corners of each panel.

mocline may play an important role in the phase locking of ENSO to AC. In order to take into account of these effects, we modified the CZ model in the following two aspects.

First, the seasonally varying part of the wind anomalies in the western Pacific was added to the CZ atmospheric model. For this purpose, an empirical atmosphere model was first constructed by applying SVD (singular value decomposition) to the observed surface wind and SST anomalies. The seasonal dependence of anomalous wind response to given SST anomalies was captured by the SVD modes computed using SST and wind anomalies that are stratified by calendar month. Thus, the empirical atmosphere model provides both season-independent wind anomalies (the annual mean SVD modes) and season-dependent wind anomalies (the annually varying SVD modes). In the MOD-CZ model, only the season-dependent components in the western Pacific (west of the dateline) were added to the wind anomalies computed from the original CZ atmosphere model. To avoid the discontinuity, a longitude-dependent weighting function was applied to the empirical wind anomalies, which decreases from unit at the date line to zero at 160°W. As shown in Fig. 3c, the western Pacific anomalous winds in the MOD-CZ model were significantly improved.

Second, the basic-state thermocline depth was derived from the CZ ocean model forced by the corresponding specified basic-state surface winds. In this way, the basic-state thermocline depth is dynamically consistent with the basic-state surface winds and model dynamics. As shown in Fig. 4, the east–west slope of the mean thermocline depth along the equator is flatter than that used in the original CZ model. However, the seasonal variation of the basic-state thermocline depth is significant (Fig. 4b). The annual range of the thermocline depth is smaller than that estimated by Wang et al. (2000a) using National Centers for Environmental Prediction (NCEP) Ocean Data Assimilation System reanalysis data. This discrepancy may be due to the differences in the wind stress forcing and the model dynamics. Comparing the sea level height obtained from the NCEP ocean assimilation data (Ji et al. 1995) (Fig. 4c) and the simulated thermocline depth (Fig. 4b) shows that the annual variations of the two fields in the eastern and central Pacific bear close similarity, although the phase of the simulated thermocline depth leads that of the sea level by about 1 month.

We first run the CZ model ($\mu = 1.2$) with the new mean thermocline depth but without seasonal variation. All other basic-state parameters are fixed at the annual cycle. As shown in Fig. 8a, the El Niño and La Niña peaks in this experiment (the empty bar) appear most frequently in October and July, respectively. These results are basically similar to those in the CZ model (shaded bar), except that the El Niño peaks occur about 1 month earlier than those in the CZ model. In the second experiment, the seasonal variation of the western

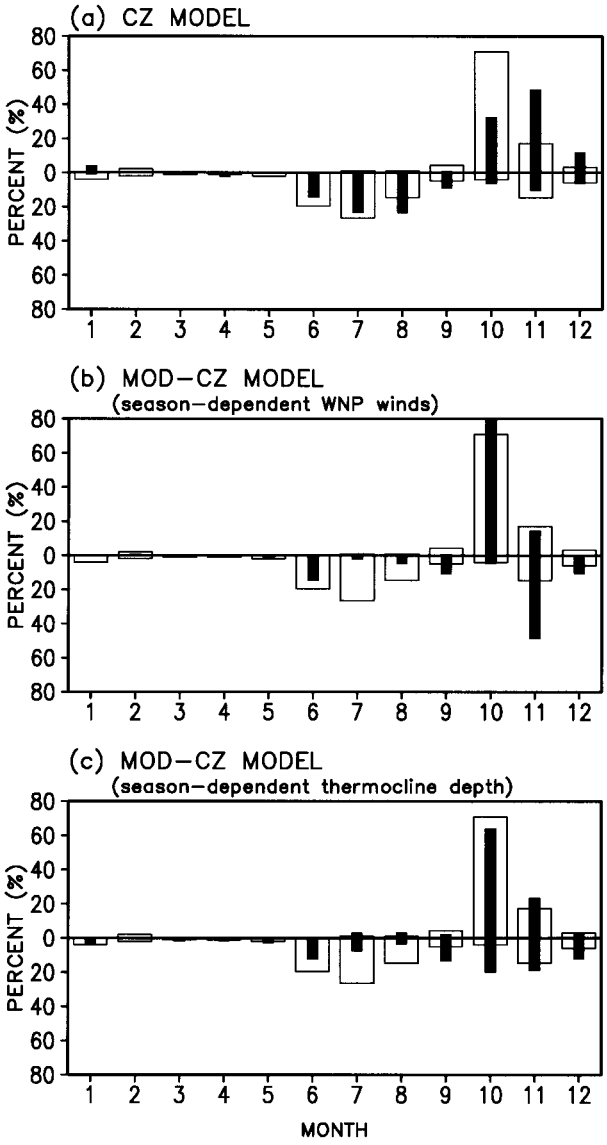

FIG. 8. Histograms showing the rate of occurrence of El Niño (above the zero line) and La Niña (below the zero line) peaks in the model as a function of calendar month. In all panels the blank bar is derived from a slightly modified CZ model run with the basic-state thermocline depth varying in both zonal and meridional directions. The filled bars are, respectively, (a) derived from the standard CZ model run, (b) from a CZ model with a modification of the western Pacific wind anomalies, and (c) from a CZ model with a modification for the seasonally varying basic-state thermocline depth.

Pacific surface wind anomalies is also included in the model (the shaded bars in Fig. 8b). The El Niño peaks prefer to occur in the same month as those in the run without seasonal effect of the western North Pacific wind (empty bars), and the La Niña peaks appear mostly in November, indicating a positive impact of the western Pacific wind anomalies. In the third experiment, the seasonal variations of the basic-state thermocline depth are included in the model (the shaded bars in Fig. 8c). In

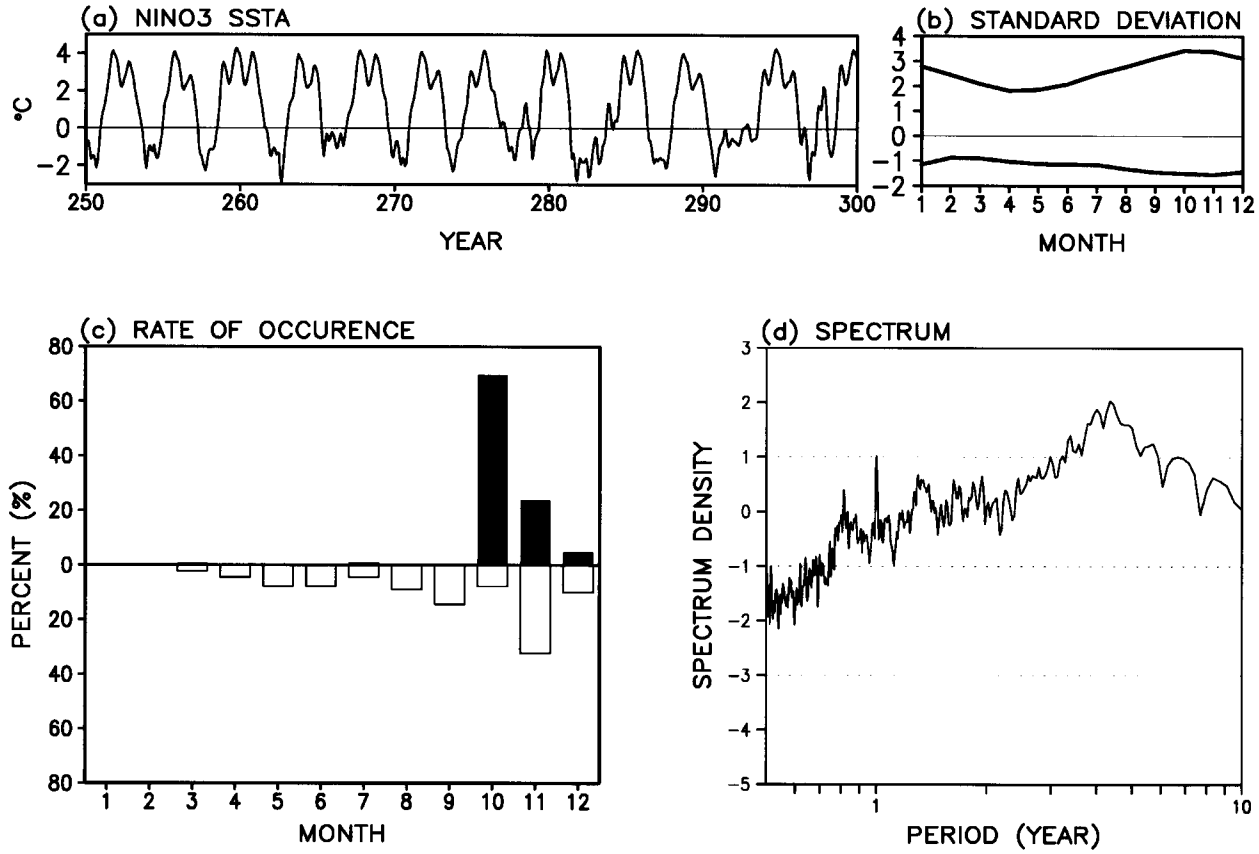

FIG. 9. (a)–(c) The same as in Figs. 2a–c, respectively, except for the modified Cane–Zebiak model. (d) Spectral density distribution obtained from Niño-3 SST anomaly shown in (a).

this experiment, both the El Niño and La Niña peaks preferably occur in October and November. The combined seasonal effects of the mean thermocline depth and the western Pacific surface wind improve ENSO phase locking to the AC.

Now, we run MOD-CZ model in which both the seasonal effects of the surface winds in the western Pacific and the basic-state thermocline depth are applied along with all other basic-state parameters that vary seasonally. The results exhibit a slightly more realistic phase locking behavior (Fig. 9c). In this experiment, as in the previous experiments, we have increased the coupling coefficient by 20% ($\mu = 1.2$) to avoid damping oscillation. The increase of the coupling coefficient slightly shortened the ENSO period. As shown in Fig. 9c, both El Niño and La Niña attain a maximum predominately in October and November, respectively. Overall, the MOD-CZ model improves the phase-locking behavior. Other ENSO characteristics are also similar to those in the original CZ model (Fig. 2) and the observation (Fig. 1). The dominant oscillation period is about 4 yr with the other two peaks at 9 months and 1 yr (Fig. 9d). The 9-month period reflects the timescale of the thermocline adjustment in the Pacific basin due to equatorial waves. The 1-yr period originates from the prescribed seasonally varying basic state.

Using MOD-CZ model ($\mu = 1.2$), we further perform sensitivity experiments to isolate the seasonal effect due to each basic-state parameter. First, all basic-state parameters are fixed at the AM values except for one having AC. Inspection of the results shown in Figs. 10a–f suggests that seasonal cycle of all basic-state parameters favors the lock of El Niño peak to the end of the calendar year (from October to February). On the other hand, only the seasonal variations of the surface winds and thermocline depth favor the occurrence of La Niña peaks toward the end of the calendar year. We should keep in mind that the seasonal variation of winds include the effect of the seasonal variation of the western Pacific wind anomalies, and the AC of thermocline depth is consistent with the AC of the surface winds. This set of experiments explains why in the CZ model the La Niña phase locks to boreal summer, whereas in the modified CZ model the La Niña phase locks to the end of the calendar year. The two additional seasonal effects added to the CZ model play an essential role in accounting for the difference.

To further examine the role of individual parameters,

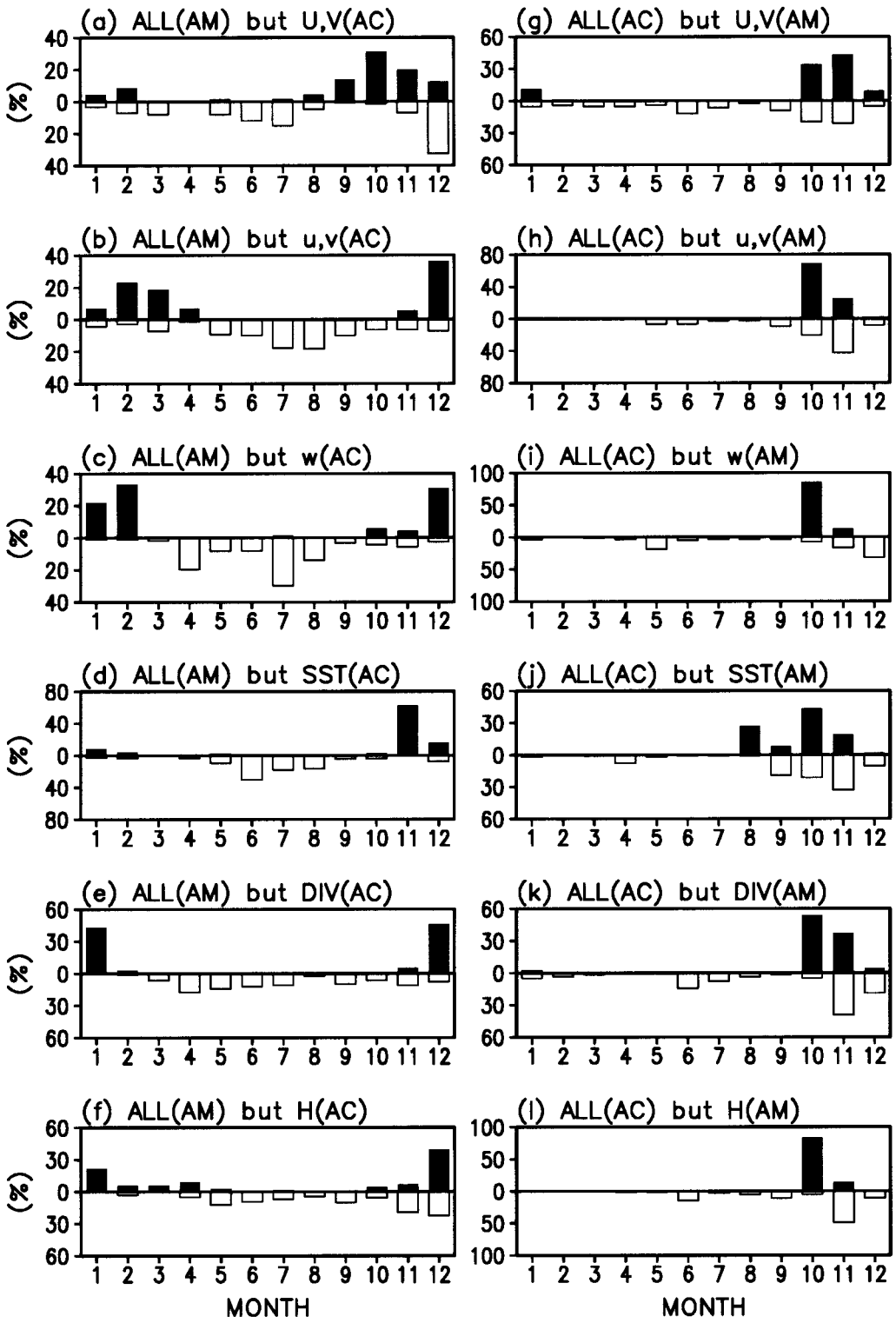

FIG. 10. Histograms showing the rate of occurrence of El Niño (filled bar) and La Niña (blank bar) peaks obtained from the modified Cane–Zebiak model. (a)–(f) All basic states are fixed as the annual mean except one variable has the annual cycle, which is the (a) surface winds, (b) currents, (c) upwelling, (d) SST, (e) surface wind divergence, and (f) thermocline depth. (g)–(l) All basic states are fixed as the annual cycle except one variable has no annual cycle, which is the (g) surface winds, (h) currents, (i) upwelling, (j) SST, (k) surface wind divergence, and (l) thermocline depth.

another set of experiments was performed in which all basic-state variables include an AC, except that one of them is fixed at its AM. If a basic-state variable specified as AM acts as a necessary factor, one would expect that without its AC, the phase locking should be weakened or destroyed. The results presented in Figs. 10g–l show that both the El Niño and La Niña peaks in these sensitivity experiments appear during October–November similar to those in the control experiment of the MOD-CZ model. Thus, removing of the seasonal cycle of any single variable does not influence significantly the ENSO phase locking. This implies that the phase-locking behavior is not dominated by the seasonal effect of any individual component of the basic state. The combined effects of two or more variations of basic-state parameters are responsible for the ENSO phase locking to AC in the MOD-CZ model.

4. Concluding remarks and discussion

Observed El Niño and La Niña peaks tend to occur in boreal winter. In the standard CZ model, the peaks of El Niño appear during boreal winter but those of La Niña appear in boreal summer. Using the CZ model, Tziperman et al. (1997) showed that the phase locking of El Nino's peak is dominated by the basic-state wind divergence that is associated with the seasonal movement of the tropical convergence zone. Although the seasonal effect of the tropical convergence zone favors the El Niño peaking in boreal winter as had been shown by Tziperman et al. (1997), it also tends to lock the La Niña peaks to boreal summer (see Fig. 6). In this study, this inconsistence between the CZ model and observation in terms of the phase locking of La Niña was overcome by including two additional seasonal effects in the CZ model.

There are two important factors, which might affect ENSO phase locking, missing in the CZ model. One is the annual variation in the mean thermocline depth, which can affect SST through changing subsurface water temperature. The other is the western Pacific wind anomaly that exhibits significant seasonality. In boreal winter (summer), anticyclonic (cyclonic) wind anomalies prevail corresponding to positive SST anomalies in the eastern Pacific. The MOD-CZ model includes the seasonal variation of the surface wind anomalies in the western Pacific and the annual cycle of the mean thermocline depth. The phase-locking behavior in the MOD-CZ model is improved. Results indicate that the seasonal reversal of the atmospheric circulation in western Pacific and the seasonal variation of the basic-state thermocline depth are essential factors for the preferred phase locking of both El Niño and La Niña to the end of the calendar year.

Wang et al. (1999b) found that the surface wind variation in the western North Pacific plays a critical role in the turnabout of ENSO cycles. It was shown that prior to the mature phase of El Niño (La Niña), an anomalous surface anticyclone (cyclone) rapidly builds over the Philippine Sea. The anticyclonic anomalies can be maintained throughout the ensuing winter and spring by a positive wind–evaporation feedback in the following manner. In the cold season from October to May, the climatological mean winds are northeasterlies over the western North Pacific; an anomalous anticyclone superposed on the mean circulation would increase the total wind speed to the southeast of the anticyclone, thus increasing evaporation and entrainment cooling and decreasing SST. On the other hand, the cold SST anomalies would suppress local convective heating, inducing a Rossby wave response, which enhances the anomalous anticyclone. To the south of the Philippine anticyclone, the equatorial easterly anomalies may elevate the thermocline and excite equatorial Kelvin waves propagating into the eastern Pacific, providing a negative feedback to the eastern Pacific warming. Because the air–sea interaction depends on boreal cold season mean surface winds, this turnabout mechanism favors the El Niño maturing at the end of the calendar year. A similar argument applies to the turnabout of a La Niña event.

How does the annual cycle of the thermocline depth affect the ENSO phase locking? As shown in Fig. 4b, the seasonal variations of the mean thermocline depth are significant almost across the entire equatorial Pacific. It is speculated that the seasonal variation of the thermocline in the eastern Pacific plays a more important role in ENSO phase locking. In order to test this hypothesis, we have repeated the slightly modified CZ model experiment with the seasonal variation of the basic-state thermocline depth, but first allow its seasonal variation only in the eastern Pacific (east of 125°W; Fig. 11a) and then, only in the central–western Pacific (west of 125°W; Fig. 11b). As shown in Fig. 11, the calendar months when the El Niño peaks occur are nearly the same (i.e., October) in both experiments. However, the La Niña peaks in the first experiment tend to more frequently occur in October–November while those in the second experiment occur in June–July, indicating that the phase locking of the La Niña peaks in the MOD-CZ model to the boreal cold season is attributed to the seasonal variation of the basic-state thermocline depth in the eastern Pacific. This suggests that the eastern Pacific mean thermocline deepening in boreal summer and shoaling in boreal fall favor La Niña turnaround in late fall through regulating local air–sea interaction. During the late development stage of a cold event, westerly anomalies develop in the eastern Pacific, which act as a negative feedback to favor turnabout of the cold event. Summer deepening and fall shoaling of thermocline would weaken the local air–sea interaction via vertical temperature advection in summer but enhance it in fall. Therefore, the weakening of the negative feedback in summer and enhancement of the negative feedback in fall favor La Niña turnabout occurring later in the calendar year.

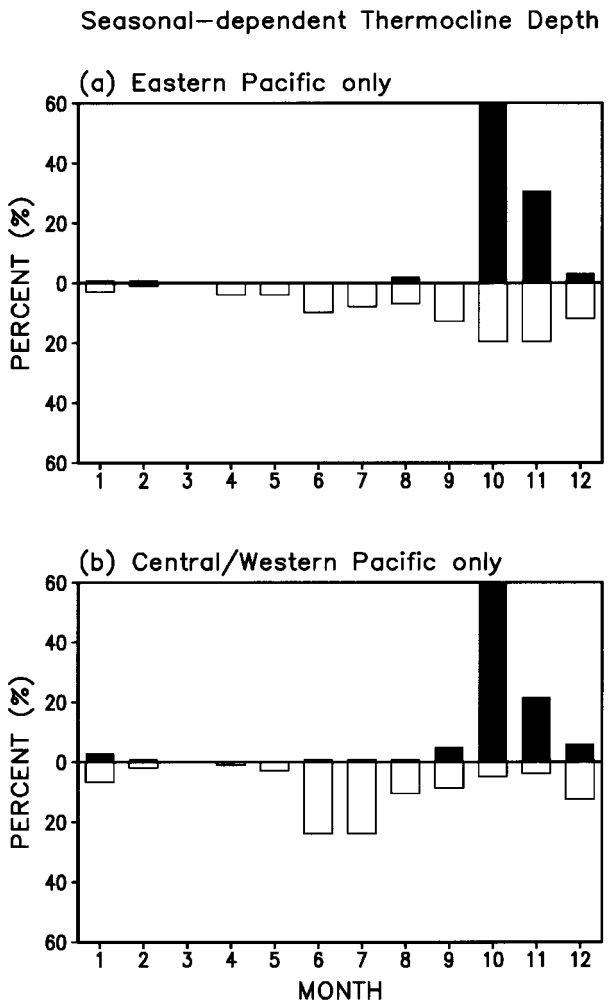

FIG. 11. Histograms showing the rate of occurrence of El Niño (above the zero line) and La Niña (below the zero line) peaks derived from a slightly modified CZ model run (coupling coefficient μ = 1.2) with a modification for the seasonally varying basic-state thermocline depth as a function of calendar month. The seasonal-dependent thermocline depth is given in (a) the eastern Pacific only, and (b) the central-western Pacific only.

In view of the limitations of the simplicity of the coupled models, the understanding gained from the present study needs further verification using models with more complete physics.

Acknowledgments. Soon-Il An has been supported by Frontier Research System for Global Change through its sponsorship of the International Pacific Research Center. Bin Wang acknowledges supports from OGP/NOAA through GOALS and PACS programs. We thank Diane Henderson for her careful reading and editing of the manuscript.

REFERENCES

An, S.-I., and B. Wang, 2000: Interdecadal change of the structure of the ENSO mode and its impact on the ENSO frequency. *J. Climate,* **13,** 2044–2055.

Cane, M. A., and S. E. Zebiak, 1985: A theory for El Niño and the Southern Oscillation. *Science,* **228,** 1084–1087.

——, ——, and S. C. Dolan, 1986: Experimental forecasts of El Niño. *Nature,* **321,** 827–832.

Chang, P., B. Wang, T. Li, and L. Ji, 1994: Interactions between the seasonal cycle and the Southern Oscillation: Frequency entrainment and chaos in an intermediate coupled ocean–atmosphere model. *Geophys. Res. Lett.,* **21,** 2817–2820.

——, ——, and ——, 1995: Interactions between the seasonal cycle and El Niño–Southern Oscillation in an intermediate coupled ocean–atmosphere model. *J. Atmos. Sci.,* **52,** 2353–2372.

Chen, D., M. A. Cane, S. E. Zebiak, and A. Kaplan, 1998: The impact of sea level data assimilation on the Lamont model prediction of the 1997/98 El Niño. *Geophys. Res. Lett.,* **25,** 2837–2840.

Deser, C., and J. M. Wallace, 1990: Large-scale atmospheric circulation features of warm and cold episodes in the Tropical Pacific. *J. Climate,* **3,** 1254–1281.

Goswami, B. N., and J. Shukla, 1993: Aperiodic variability in the Cane–Zebiak model: A diagnostic study. *J. Climate,* **6,** 628–638.

Harrison, D. E., and G. A. Vecchi, 1999: On the termination of El Niño. *Geophys. Res. Lett.,* **26,** 1593–1596.

Ji, M., A. Leetmaa, and J. Derber, 1995: An ocean analysis system for seasonal to interannual climate studies. *Mon. Wea. Rev.,* **123,** 460–481.

Jin, F.-F., 1996: Tropical ocean–atmosphere interaction, the Pacific cold tongue, and the El Niño–Southern Oscillation. *Science,* **274,** 76–78.

——, and D. J. Neelin, 1993: Modes of interannual tropical ocean–atmosphere interaction—A unified view. Part I: Numerical results. *J. Atmos. Sci.,* **50,** 3477–3503.

——, ——, and M. Ghil, 1994: El Niño on the devil's staircase: Annual subharmonic steps to chaos. *Science,* **264,** 70–72.

Kaplan, A., M. Cane, Y. Kushnir, A. Clement, M. Blumenthal, and B. Rajagopalan, 1998: Analyses of global sea surface temperature 1856–1991. *J. Geophys. Res.,* **103,** 18 567–18 589.

Mantua, N. J., and D. S. Battisti, 1995: Aperiodic variability in the Zebiak–Cane coupled ocean–atmosphere model: Air–sea interactions in the western equatorial Pacific. *J. Climate,* **8,** 2897–2927.

Ropelewski, C. F., and M. S. Halpert, 1987: Global and regional scale precipitation patterns associated with the El Niño–Southern Oscillation. *Mon. Wea. Rev.,* **115,** 1606–1626.

——, and ——, 1989: Precipitation patterns associated with the high index phase of the Southern Oscillation. *J. Climate,* **2,** 268–284.

Tziperman, E., L. Stone, M. Cane, and H. Jarosh, 1994: El Niño chaos: Overlapping of resonances between the seasonal cycle and the Pacific ocean–atmosphere oscillator. *Science,* **264,** 72–74.

——, M. A. Cane, and S. E. Zebiak, 1995: Irregularity and locking to the seasonal cycle in an ENSO-prediction model as explained by the quasi-periodic route to chaos. *J. Atmos. Sci.,* **52,** 293–306.

——, S. E. Zebiak, and M. A. Cane, 1997: Mechanisms of seasonal–ENSO interaction. *J. Atmos. Sci.,* **54,** 61–71.

——, M. A. Cane, S. E. Zebiak, Y. Xue, and B. Blumenthal, 1998: Locking of El Niño's peak time to the end of the calendar year in the delayed oscillator picture of ENSO. *J. Climate,* **11,** 2191–2199.

Wang, B., and Z. Fang, 1996: Chaotic oscillation of tropical climate: A dynamic system theory for ENSO. *J. Atmos. Sci.,* **53,** 2786–2802.

——, A. Barcilon, and Z. Fang, 1999a: Stochastic dynamics of El Niño–Southern Oscillation. *J. Atmos. Sci.,* **56,** 5–23.

——, R. Wu, and R. Lukas, 1999b: Roles of the western North Pacific wind variation in thermocline adjustment and ENSO phase transition. *J. Meteor. Soc. Japan,* **77,** 1–16.

——, ——, and ——, 2000a: Annual adjustment of the thermocline in the tropical Pacific Ocean. *J. Climate,* **13,** 596–616.

——, ——, and X. Fu, 2000b: Pacific–East Asian teleconnection: How does ENSO affect East Asian climate? *J. Climate,* **13,** 1517–1536.

Zebiak, S. E., and M. A. Cane, 1987: A model El Niño–Southern Oscillation. *Mon. Wea. Rev.,* **115,** 2262–2278.